19. Arnheim, N., Treco, D., Taylor, B. & Eicher, E. M. Distribution of ribosomal gene length variants among mouse chromosomes. *Proc. Natl Acad. Sci. USA* **79,** 4677–4680 (1982).

20. Birky, C. W. Heterozygosity, heteromorphy, and phylogenetic trees in asexual eukaryotes. *Genetics* **144,** 427–437 (1996).

21. Hosny, M., Gianinazzi-Pearson, V. & Dulieu, H. Nuclear DNA content of 11 fungal species in Glomales. *Genome* **41,** 422–428 (1998).

22. Otto, S. P. & Whitton, J. Polyploid incidence and evolution. *Annu. Rev. Genet.* **34,** 401–437 (2000).

23. Mogie, M. & Ford, H. Sexual and asexual *Taraxacum* species. *Biol. J. Linn. Soc.* **35,** 155–168 (1988).

24. Kondrashov, A. S. The asexual ploidy cycle and the origin of sex. *Nature* **370,** 213–216 (1994).

25. Swofford, D. L. PAUP: phylogenetic analysis using parsimony (and other methods). Ver. 4 (Sinauer, Sunderland, MA, 1998).

• •

Multistability in the lactose utilization network of *Escherichia coli*

Ertugrul M. Ozbudak[1]*, **Mukund Thattai**[1]*, **Han N. Lim**[1], **Boris I. Shraiman**[2] & **Alexander van Oudenaarden**[1]

[1]*Department of Physics, Massachusetts Institute of Technology, Cambridge, Massachusetts 02139, USA*
[2]*Department of Physics and the BioMAPS Institute, Rutgers University, Piscataway, New Jersey 08854, USA*

* These authors contributed equally to this work

....

Multistability, the capacity to achieve multiple internal states in response to a single set of external inputs, is the defining characteristic of a switch. Biological switches are essential for the determination of cell fate in multicellular organisms[1], the regulation of cell-cycle oscillations during mitosis[2,3] and the maintenance of epigenetic traits in microbes[4]. The multistability of several natural[1–6] and synthetic[7–9] systems has been attributed to positive feedback loops in their regulatory networks[10]. However, feedback alone does not guarantee multistability. The phase diagram of a multistable system, a concise description of internal states as key parameters are varied, reveals the conditions required to produce a functional switch[11,12]. Here we present the phase diagram of the bistable lactose utilization network of *Escherichia coli*[13]. We use this phase diagram, coupled with a mathematical model of the network, to quantitatively investigate processes such as sugar uptake and transcriptional regulation *in vivo*. We then show how the hysteretic response of the wild-type system can be converted to an ultrasensitive graded response[14,15]. The phase diagram thus serves as a sensitive probe of molecular interactions and as a powerful tool for rational network design.

The bistability of the lactose utilization network has been under investigation since 1957 (refs 16, 17). The basic components of this network have been well characterized[13], making it an ideal candidate for global analysis. The *lac* operon comprises three genes required for the uptake and metabolism of lactose and related sugars (Fig. 1): *lacZ*, *lacY* and *lacA*. *lacZ* codes for β-galactosidase, an enzyme responsible for the conversion of lactose into allolactose and subsequent metabolic intermediates. *lacY* codes for the lactose permease (LacY), which facilitates the uptake of lactose and similar molecules, including thio-methylgalactoside (TMG), a non-metabolizable lactose analogue. *lacA* codes for an acetyltransferase, which is involved in sugar metabolism. The operon has two transcriptional regulators: a repressor (LacI) and an activator (the cyclic AMP receptor protein, CRP). Inducers, among them allolactose and TMG, bind to and inhibit repression by LacI, whereas cAMP binds to and triggers activation by CRP. The concentration of cAMP drops in response to the uptake of various carbon sources, including glucose and lactose[18]; glucose uptake also interferes with LacY activity, leading to exclusion of the inducer[18]. Together these effects mediate catabolite repression—the ability of glucose to inhibit *lac* expression. Crucially, cAMP levels are not affected by TMG uptake. Therefore, the extracellular concentrations of TMG and glucose can be used to independently regulate the activities of LacI and CRP, the two *cis*-regulatory inputs of the *lac* operon[19]. However, the response of the operon must be considered within the broader context of the network. The uptake of TMG induces the synthesis of LacY, which in turn promotes further TMG uptake; the resulting positive feedback loop creates the potential for bistability[20,21].

To probe the network's bistable response, we incorporated a single copy of the green fluorescent protein gene (*gfp*) under the control of the *lac* promoter into the chromosome of *E. coli* MG1655 (Fig. 1). We placed this reporter in the chromosome rather than on a multicopy plasmid to minimize the titration of LacI molecules by extraneous LacI-binding sites. The cells also contained a plasmid encoding a red fluorescent reporter (HcRed) under the control of the galactitol (*gat*) promoter. This promoter includes a CRP-binding site, as well as a binding site for the galactitol repressor,
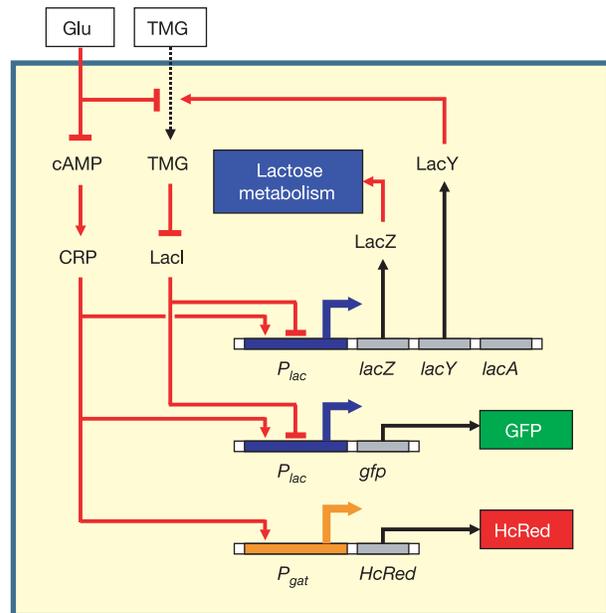

Figure 1 The lactose utilization network. Red lines represent regulatory interactions, with pointed ends for activation and blunt ends for inhibition; black arrows represent protein creation through transcription and translation, and dotted arrows represent uptake across the cell membrane. In our experiments we vary two external inputs, the extracellular concentrations of glucose and TMG, and measure the resulting levels of two fluorescent reporter proteins: GFP, expressed at the *lac* promoter, and HcRed, expressed at the *gat* promoter. LacY catalyses the uptake of TMG, which induces further expression of LacY, resulting in a positive feedback loop.

GatR. However, GatR is absent in *E. coli* MG1655 (ref. 22). Therefore, transcription at the *gat* promoter, measured by red fluorescence, is a direct measure of CRP-cAMP levels. In our experiments, we measure the response of single cells, initially in a given state of *lac* expression, to exposure to various combinations of glucose and TMG levels (Fig. 2a). It is crucial to use cells with well-defined initial states, either uninduced or fully induced, because the response of a bistable system is expected to depend on its history.

We find, in the absence of glucose, that the *lac* operon is uninduced at low TMG concentrations ($<3\,\mu M$) and fully induced at high TMG concentrations ($>30\,\mu M$) regardless of the cell's history. Between these switching thresholds, however, system response is hysteretic (history dependent): TMG levels must exceed $30\,\mu M$ to turn on initially uninduced cells but must drop below $3\,\mu M$ to turn off initially induced cells (Fig. 2b). As we approach the boundaries of this bistable region, stochastic mechanisms cause growing numbers of cells to switch from their initial states, resulting in a bimodal distribution of green fluorescence levels, with induced cells having over one hundred times the fluorescence levels of uninduced cells. This behaviour shows the importance of performing single-cell experiments, as a population-averaged measurement would have shown the mean fluorescence level to move smoothly between its low and high endpoints[2], obscuring the fact that individual cells never display intermediate fluorescence levels.

We find that the red fluorescence level is independent of cell history and of TMG concentration, showing that the observed history dependence of *lac* induction is not due to CRP. Red fluorescence levels do decrease in response to an increase in glucose concentration, ultimately dropping fivefold (Fig. 3a). There is a proportional drop in the green fluorescence levels of induced cells, reflecting the reduction in the levels of CRP-cAMP. The network continues to respond hysteretically in the presence of glucose, but higher levels of TMG are required to induce switching. By measuring system response at several glucose concentrations ranging from 0 to 1 mM, we are able to map out the complete range of glucose and TMG levels over which the system is bistable (Fig. 2c). This is the phase diagram of the wild-type lactose utilization network.

The switching boundaries of this phase diagram correspond to special conditions of network dynamics. By imposing these conditions within a mathematical model of the *lac* system, we are able to use the phase diagram as a quantitative probe of molecular processes in living single cells (see Supplementary Information).

The green fluorescence levels at each glucose and TMG concentration can be written as a function of three parameters: α, β and ρ. The maximal activity, α, is the *lac* expression level that would be obtained if every repressor molecule were inactive. The repression factor, ρ, gives the ratio of maximal to basal activities, the latter being the expression level that would be obtained if every repressor molecule were active. The transport rate, β, gives the TMG uptake rate per LacY molecule. We find that α is directly proportional to the red fluorescence level (Fig. 3b), demonstrating that the *lac* and *gat* promoters respond identically to CRP-cAMP. By contrast, α is essentially independent of TMG levels, suggesting that LacI and CRP bind independently to the *lac* operator site. We find the repression factor ρ to be 170 ± 30 regardless of the glucose and TMG levels (Fig. 3c). This confirms a strong prediction of our model—that ρ should be a function of the LacI concentration alone. Assuming an effective LacI concentration in the nanomolar range[13], this value of ρ implies a dissociation constant between LacI and its major DNA-binding site of about 10^{-10} to 10^{-11} M, which is consistent with reported values[23].

The transport rate β is a product of two terms. The first term, β_T, which represents the TMG uptake rate per active LacY molecule, is purely a function of extracellular TMG levels (Fig. 3d). By fitting β_T to a hyperbola, we find that the half-saturation concentration for TMG uptake is $680 \pm 25\,\mu M$, which agrees with previous measurements[24]. The second term, β_G, which represents the fraction of LacY molecules that are active, is purely a function of extracellular glucose levels, reflecting the inducer-exclusion effect[18]. This allows us to separate catabolite repression into its constituent parts (Fig. 3e). We find that by lowering CRP-cAMP levels glucose reduces operon expression by 80%, whereas by inactivating LacY molecules it reduces TMG uptake by 35%. However, the network's positive feedback architecture amplifies these effects, resulting in the observed hundred-fold difference in *lac* expression levels between induced and uninduced cells. This type of global information would be extremely difficult to obtain using standard molecular-genetic techniques and *in vitro* biochemical assays. Our approach allows us to study the wild-type network in its entirety rather than isolated from other cellular systems or broken up into simpler subcomponents.

The phase diagram of the wild-type network (Fig. 2c) shows that *lac* induction always takes place hysteretically, with cells increasing their expression levels discontinuously as a switching threshold is
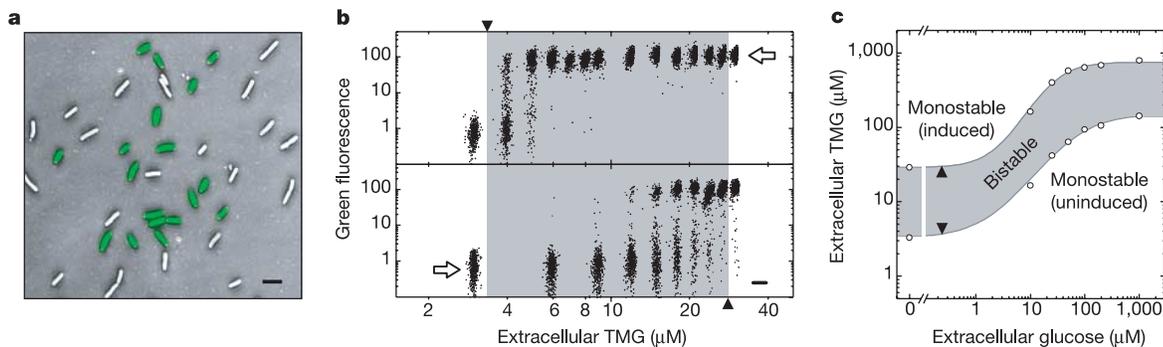

Figure 2 Hysteresis and bistability in single cells. **a**, Overlayed green fluorescence and inverted phase-contrast images of cells that are initially uninduced for *lac* expression, then grown for 20 h in 18 μM TMG. The cell population shows a bimodal distribution of *lac* expression levels, with induced cells having over one hundred times the green fluorescence of uninduced cells. Scale bar, 2 μm. **b**, Behaviour of a series of cell populations, each initially uninduced (lower panel) or fully induced (upper panel) for *lac* expression, then grown in media containing various amounts of TMG. Scatter plots show log(green fluorescence) versus log(red fluorescence) for about 1,000 cells in each population. Each scatter plot is centred at a position that indicates the underlying TMG

concentration. The scale bar represents variation in red fluorescence by a factor of 10. White arrows indicate the initial states of the cell populations in each panel. The TMG concentration must increase above 30 μM to turn on initially uninduced cells (up arrow), whereas it must decrease below 3 μM to turn off initially induced cells (down arrow). The grey region shows the range of TMG concentrations over which the system is hysteretic. **c**, The phase diagram of the wild-type lactose utilization network. When glucose is added to the medium, the hysteretic region moves to higher levels of TMG. At each glucose level, the lower (down arrow) and upper (up arrow) switching thresholds show those concentrations of TMG at which less than 5% of the cells are in their initial states.

reached. However, our theoretical phase diagram (Fig. 4d) suggests that system response could also occur in a graded fashion, with the expression levels of individual cells moving continuously between low and high values. Such a response is predicted to occur when the degree of operon repression, ρ, is decreased below wild-type levels. Guided by this prediction, we sought to elicit a graded response from the *lac* system. We constructed two new strains, one containing a plasmid with an average copy number of 4, and the other containing a plasmid with an average copy number of 25. Each plasmid carried a single copy of the *lac* promoter. The introduction of extra LacI-binding sites had the expected titrating effect, reducing the effective LacI concentration and causing a drop in the operon-repression factor ρ from its wild-type value of 170, to 50 in the cells with 4 plasmids, and 5 in the cells with 25 plasmids. Graded behaviour is expected to occur below a repression factor of nine, and this is precisely what we observe: cells with a repression factor of 50 have a discontinuous hysteretic response similar to that of the original cells (Fig. 4b), whereas cells with a repression factor of 5 show a continuous graded response (Fig. 4c).

The ability of a single system to produce both binary and graded responses has previously been observed but not explained[15]. Here we present a general mechanism by which this may be achieved and experimentally validate this mechanism in the context of a natural biological system, the lactose utilization network. We show that the observed change from the wild-type binary response to the engineered graded response should be interpreted as a shift between different parts of a unified phase diagram. In this respect, the behaviour of the *lac* system closely resembles that of thermo-

dynamic systems[11]: the discontinuous transition from low to high induction is analogous to a first-order phase transition such as evaporation in a liquid–gas system, with chemical noise instead of thermal noise driving stochastic transitions between these states[8,25]. The shift from a hysteretic to a graded response is analogous to a second-order phase transition across a critical point. More complex transitions, such as those between different types of multistability[26] or between stable and oscillatory behaviour[27,28], can be similarly analysed. The response of any natural network may be regarded as a single realization in a vast but structured space of possible
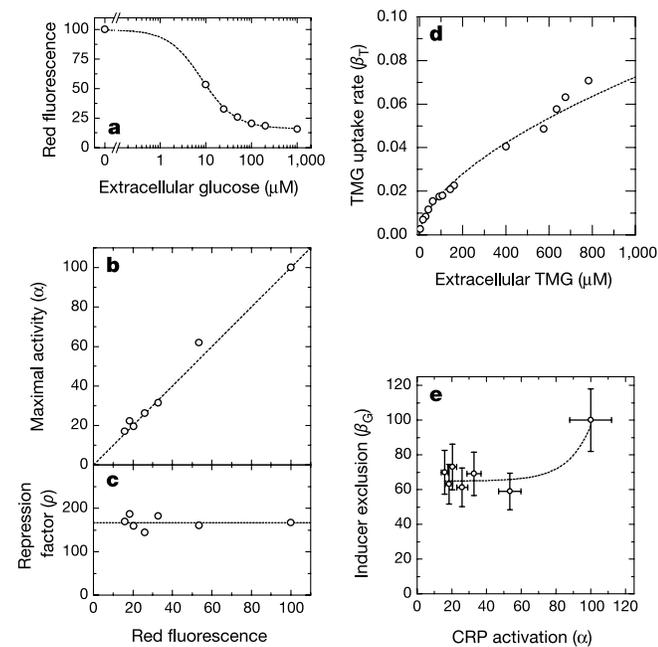

Figure 4 Hysteretic and graded responses. **a–c**, Histograms of log(green fluorescence) for cell populations that are initially uninduced, then grown in media containing 1 mM glucose and various levels of TMG (indicated in μM on each panel). **a**, Response of the wild-type network. **b**, **c**, Response of the network after the introduction of extraneous LacI-binding sites on a 4-copy plasmid (**b**) and a 25-copy plasmid (**c**). The response of the wild-type and the 4-copy cells is hysteretic, whereas that of the 25-copy cells is graded. Bimodal histograms are shown in grey panels. **d**, Theoretical phase diagram of the lactose utilization network. It is possible to move from an uninduced to an induced state either hysteretically (grey region) or in a graded manner (white region). For the wild-type network we show the fitted parameters as white dots. For all three networks, we indicate the estimated operon-repression factors by vertical lines. The region of bistability grows smaller as the repression factor is decreased, eventually reaching a critical point (C) at a repression factor of 9. Graded behaviour is predicted to occur beyond this cusp.
e, The mean green fluorescence level of each cell population in Fig. 4c is shown as a function of the TMG concentration. The response is highly sigmoidal (Hill coefficient ≈ 6) owing to positive feedback.

Figure 3 Single-cell *in vivo* measurement of network parameters. **a**, The mean red fluorescence level of each cell population is independent of its history but decreases with increasing glucose concentrations. **b–d**, Model parameters are extracted by fitting to measured fluorescence values at the switching thresholds. **b**, The maximal promoter activity, α, increases linearly with red fluorescence. **c**, The operon repression factor, ρ, is constant. **d**, The TMG uptake rate per active permease, β_T, increases with extracellular TMG levels. The dashed line shows a power-law fit with an exponent of 0.6. The data can also be fitted using a hyperbola, giving a half-saturation concentration of $680\,\mu$M. **e**, The elements of catabolite repression. At each glucose concentration, we show the transport activity of LacY molecules (β_G, measuring inducer exclusion) versus the transcriptional activity of the *lac* operon (α, measuring CRP activation). We see that permease activity drops rapidly as glucose is added, falling to 65% of its maximal value. Operon activity drops more gradually, but falls to 20% of its maximal value. Error bars were determined by propagating the experimental error in measured fluorescence values.
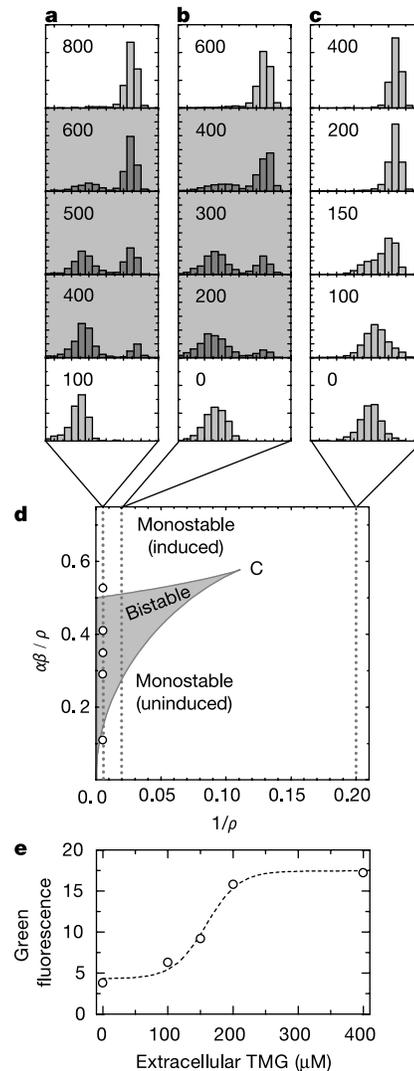
©2004 **Nature Publishing Group**

responses. By experimentally probing this space, we are able to gain quantitative insight into the architecture, dynamics and design constraints of biological systems. ☐

Methods

Bacterial strains and plasmids

The *gfp* gene under the control of the wild-type *lac* promoter, obtained from plasmid pGFPmut3.1 (Clontech), was inserted into the chromosome of *E. coli* MG1655 at the lambda insertion site using the λ-InCH technique[29] to produce the strain MUK21. The *gat* promoter was amplified from the *E. coli* MG1655 chromosome by polymerase chain reaction using primers flanking the 2,175,231–2,175,531 chromosomal region. The *HcRed* gene was obtained from pHcRed1–C1 (Clontech) and was placed under the control of the *gat* promoter into a plasmid with a ColE1 replication origin, which was transformed into MUK21 cells to obtain the strain ERT113. All measurements of wild-type network response were conducted in this strain. Two additional strains with *lac* operon repression factors at lower levels than in the wild-type were constructed by transforming MUK21 cells with multicopy plasmids, each incorporating a single copy of the *lac* promoter. The strain MUK21-pSC101* contains plasmids with a pSC101* replication origin (average copy number 4), and the strain MUK21-p15A contains plasmids with a p15A replication origin (average copy number 25)[30].

Growth conditions and media

Cells were grown at 37 °C in M9 minimal medium with succinate as the main carbon source, supplemented with varying amounts of glucose and TMG. Master cultures with cells induced for *lac* expression were prepared by overnight growth in 1 mM TMG, and master cultures with uninduced cells by overnight growth in the absence of TMG. During each experimental run, cells were transferred from these master cultures into media containing specified amounts of glucose and TMG. They were subsequently grown for 20 additional hours before they were harvested for measurement. The transfer volume was calculated to produce extremely low final cell densities ($OD_{600} \sim 0.001$), thereby preventing the depletion of glucose and TMG from the medium. Cells were concentrated by filtration and centrifugation, and the resulting pellet was resuspended in 2.5 μl of the growth medium to prepare a microscope slide.

Data acquisition

Green and red fluorescence values of single cells were measured using a Nikon TE2000 microscope with automated stage and focus. For each experiment, images of about 1,000 cells on each slide were collected using a cooled back-thinned CCD camera (Micromax, Roper Scientific). These images were analysed using Metamorph (Universal Imaging) to obtain the average fluorescence of each cell above the fluorescence background.

Data analysis

For each glucose concentration, the fraction of cells in the induced state was determined as a function of TMG concentration, and the switching thresholds (defined as the TMG concentrations at which less than 5% of the cells are in their initial states) were obtained by interpolation. We estimated the green fluorescence values of the induced (high) and uninduced (low) subpopulations at each switching threshold by averaging over two neighbouring TMG concentrations. At each threshold, the high fluorescence was a linear function of the low fluorescence, with a small positive intercept comparable to the autofluorescence of *E. coli* MG1655 cells. We interpreted this intercept as the autofluorescence of the ERT113 strain. The repression factors for the MUK21-pSC101* and MUK21-p15A strains were estimated by taking the ratio of fully induced to uninduced fluorescence levels, assuming that these strains had the same autofluorescence background as ERT113.

1. Ferrell, J. E. Jr & Machleder, E. M. The biochemical basis of an all-or-none cell fate switch in *Xenopus* oocytes. *Science* **280**, 895–898 (1998).
2. Pomerening, J. R., Sontag, E. D. & Ferrell, J. E. Jr Building a cell cycle oscillator: hysteresis and bistability in the activation of Cdc2. *Nature Cell Biol.* **5**, 346–351 (2003).
3. Sha, W. *et al.* Hysteresis drives cell-cycle transitions in *Xenopus laevis* egg extracts. *Proc. Natl Acad. Sci. USA* **100**, 975–980 (2003).
4. Hernday, A., Braaten, B. A. & Low, D. The mechanism by which DNA adenine methylase and PapI activate the pap epigenetic switch. *Mol. Cell* **12**, 947–957 (2003).
5. Blauwkamp, T. A. & Ninfa, A. J. Physiological role of the GlnK signal transduction protein of *Escherichia coli*: survival of nitrogen starvation. *Mol. Microbiol.* **46**, 203–214 (2002).
6. Siegele, D. A. & Hu, J. C. Gene expression from plasmids containing the araBAD promoter at subsaturating inducer concentrations represents mixed populations. *Proc. Natl Acad. Sci. USA* **94**, 8168–8172 (1997).
7. Gardner, T. S., Cantor, C. R. & Collins, J. J. Construction of a genetic toggle switch in *Escherichia coli*. *Nature* **403**, 339–342 (2000).
8. Isaacs, F. J., Hasty, J., Cantor, C. R. & Collins, J. J. Prediction and measurement of an augoregulatory genetic module. *Proc. Natl Acad. Sci. USA* **100**, 7714–7719 (2003).
9. Becskei, A., Seraphin, B. & Serrano, L. Positive feedback in eukaryotic gene networks: cell differentiation by graded to binary response conversion. *EMBO J.* **20**, 2528–2535 (2001).
10. Ferrell, J. E. Jr Self-perpetuating states in signal transduction: positive feedback, double-negative feedback and bistability. *Curr. Opin. Cell Biol.* **14**, 140–148 (2002).
11. Ma, S.-K. *Modern Theory of Critical Phenomena* (Perseus Books, Reading, Massachusetts, 1976).
12. Strogatz, S. H. *Nonlinear Dynamics and Chaos* (Perseus Books, Reading, Massachusetts, 1994).
13. Müller-Hill, B. *The Lac Operon: A Short History of a Genetic Paradigm* (Walter de Gruyter, Berlin, 1996).
14. Louis, M. & Becskei, A. Binary and graded responses in gene networks. *Science STKE* [online],

30 July 2002 (doi:10.1126/stke.2002.143.pe33).
15. Biggar, S. R. & Crabtree, G. R. Cell signaling can direct either binary or graded transcriptional responses. *EMBO J.* **20**, 3167–3176 (2001).
16. Novick, A. & Weiner, M. Enzyme induction as an all-or-none phenomenon. *Proc. Natl Acad. Sci. USA.* **43**, 553–566 (1957).
17. Cohn, M. & Horibata, K. Inhibition by glucose of the induced synthesis of the β-galactoside-enzyme system of *Escherichia coli*: Analysis of maintenance. *J. Bacteriol.* **78**, 601–612 (1959).
18. Stulke, J. & Hillen, W. Carbon catabolite repression in bacteria. *Curr. Opin. Microbiol.* **2**, 195–201 (1999).
19. Setty, Y., Mayo, A. E., Surette, M. G. & Alon, U. Detailed map of a *cis*-regulatory input function. *Proc. Natl Acad. Sci. USA* **100**, 7702–7707 (2003).
20. Griffith, J. S. Mathematics of cellular control processes II: Positive feedback to one gene. *J. Theor. Biol.* **20**, 209–216 (1968).
21. Tyson, J. J. & Othmer, H. G. The dynamics of feedback control circuits in biochemical pathways. *Prog. Theor. Biol.* **5**, 1–62 (1978).
22. Nobelmann, B. & Lengeler, J. W. Molecular analysis of the *gat* genes from *Escherichia coli* and of their roles in galactitiol transport and metabolism. *J. Bacteriol.* **178**, 6790–6795 (1996).
23. Oehler, S., Eismann, E. R., Kramer, H. & Müller-Hill, B. The three operators of the *lac* operon cooperate in repression. *EMBO J.* **9**, 973–979 (1990).
24. Chung, J. D. & Stephanopoulos, G. On physiological multiplicity and population heterogeneity of biological systems. *Chem. Eng. Sci.* **51**, 1509–1521 (1996).
25. Kepler, T. B. & Elston, T. C. Stochasticity in transcriptional regulation: origins, consequences, and mathematical representations. *Biophys. J.* **81**, 3116–3136 (2001).
26. Thattai, M. & Shraiman, B. I. Metabolic switching in the sugar phosphotransferase system of *Escherichia coli*. *Biophys. J.* **85**, 744–754 (2003).
27. Atkinson, M. R., Savageau, M. A., Myers, J. T. & Ninfa, A. J. Development of genetic toggle circuitry exhibiting toggle switch or oscillatory behavior in *Escherichia coli*. *Cell* **113**, 597–607 (2003).
28. Smolen, P., Baxter, D. A. & Byrne, J. H. Frequency selectivity, multistability, and oscillations emerge from models of genetic regulatory systems. *Am. J. Physiol.* **43**, C531 (1998).
29. Boyd, D., Weiss, D. S., Chen, J. C. & Beckwith, J. Towards single-copy gene expression systems making gene cloning physiologically relevant: lambda InCh, a simple *Escherichia coli* plasmid-chromosome shuttle system. *J. Bacteriol.* **182**, 842–847 (2000).
30. Lutz, R. & Bujard, H. Independent and tight regulation of transcriptional units in *Escherichia coli* via the LacR/O, the TetR/O and AraC/I1-I2 regulatory elements. *Nucleic Acids Res.* **25**, 1203–1210 (1997).

....

Unique astrocyte ribbon in adult human brain contains neural stem cells but lacks chain migration

Nader Sanai[1,2], **Anthony D. Tramontin**[1,2], **Alfredo Quiñones-Hinojosa**[1], **Nicholas M. Barbaro**[1], **Nalin Gupta**[1], **Sandeep Kunwar**[1], **Michael T. Lawton**[1], **Michael W. McDermott**[1], **Andrew T. Parsa**[1], **José Manuel-García Verdugo**[3], **Mitchel S. Berger**[1] **& Arturo Alvarez-Buylla**[1,2]

[1]*Department of Neurological Surgery and Brain Tumor Research Center, and* [2]*Developmental Stem Cell Biology Program, University of California San Francisco, San Francisco, California 94143, USA* [3]*Instituto Cavanilles, University of Valencia, 46100, Spain*

....

The subventricular zone (SVZ) is a principal source of adult neural stem cells in the rodent brain, generating thousands of olfactory bulb neurons every day[1]. If the adult human brain contains a comparable germinal region, this could have considerable implications for future neuroregenerative therapy. Stem cells have been isolated from the human brain[2–7], but the identity, organization and function of adult neural stem cells in the